Journal of Power Sources 245 (2014) 1005–1013

Contents lists available at ScienceDirect

Journal of Power Sources

journal homepage: www.elsevier.com/locate/jpowsour

Synthesis of novel cardo poly(arylene ether sulfone)s with bulky and rigid side chains for direct methanol fuel cells

Jifu Zheng [a], Jing Wang [a,b], Suobo Zhang [a,*], Ting Yuan [c], Hui Yang [c,**]

[a] Key Laboratory of Polymer Ecomaterials, Changchun Institute of Applied Chemistry, Chinese Academy of Sciences, Changchun 130022, China
[b] Graduate School of Chinese Academy of Sciences, Beijing 100049, China
[c] Shanghai Institute of Microsystem and Information Technology, Shanghai Advanced Research Institute, Chinese Academy of Sciences, Shanghai 200050, China

HIGHLIGHTS

- Cardo poly(arylene ether sulfone)s membranes with bulky and rigid side chains was synthesized.
- Nanophase separated morphology with well-defined ionic clusters of 2–5 nm.
- SPES-*x* revealed high proton conductivity and low methanol permeability.
- SPES-20 exhibited superior cell performance compared with Nafion® 117.

GRAPHICAL ABSTRACT

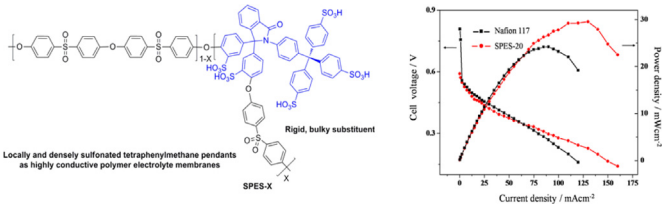

ARTICLE INFO

Article history:
Received 3 March 2013
Received in revised form
11 July 2013
Accepted 12 July 2013
Available online 20 July 2013

Keywords:
Proton exchange membrane
Sulfonated poly(arylene ether sulfone)s
Bulky and rigid side chains
Dimensional stability
Cell performance

ABSTRACT

A new series of sulfonated cardo poly(arylene ether sulfone)s (SPES-*x*) with bulky and rigid side chains have been synthesized based on a novel bisphenol monomer containing electron rich tetraphenylmethane groups. The SPES-*x* membranes show the desired characterizations such as high solubility in common organic solvents, good film-forming ability, excellent thermal and mechanical properties, and low methanol permeability. As ion exchange capacity (IEC) ranging from 1.61 to 2.14 mequiv g^{-1}, SPES-*x* membranes afford high conductivity (>0.08 S cm^{-1}) and low swelling ratio under fully hydrated state at room temperature. Their excellent properties can be attributed to the formation of the well-defined phase-separated structures and well-connected proton transport channels observed in TEM and SAXS.

Furthermore, the passive direct methanol fuel cells (DMFC) with SPES-20 membrane presents a maximum power density of 29.4 mW cm^{-2} at 25 °C, which is superior to the value of Nafion® 117.

1. Introduction

Proton exchange membrane fuel cells (PEMFCs) have attracted particular interest as alternative and environmentally friendly energy sources for both mobile and stationary applications [1–4]. The key component of PEMFCs is the proton exchange membrane (PEM), which acts as an electrolyte to transport protons from the anode to the cathode. The perfluorosulfonic acid membranes, such as Nafion®, are most used PEMs because of their superior chemical and electrochemical stability, in addition to high proton conductivity with relatively low ion exchange capacity (IEC). However, their critical drawbacks of high cost, complicated synthesis procedure, high methanol crossover, and low application temperature have stimulated extensive research into the investigation of promising new membranes for the request of industry [5].

* Corresponding author. Tel.: +86 431 85262118; fax: +86 431 85685653.
** Corresponding author. Fax: +86 21 32200534.
E-mail addresses: sbzhang@ciac.jl.cn (S. Zhang), yangh@sari.ac.cn (H. Yang).

0378-7753/$ – see front matter © 2013 Elsevier B.V. All rights reserved.
http://dx.doi.org/10.1016/j.jpowsour.2013.07.061

The majority of current research on PEMs is based on sulfonated aromatic polymers, including sulfonated poly(arylene ether sulfone)s [6,7], poly(arylene ether ketone)s [8,9], polyimides [10], poly(arylene ether nitrile)s [11], because of the high thermal and chemical stabilities, as well as excellent mechanical properties of the parent polymers.

As well known, proton conductivity is the most significant characteristic of PEMs, which correlates to IEC values, acidity of the ionic groups and morphological phase-separation. Sulfonated polymers having high IEC values usually exhibit high proton conductivity. However, high IEC usually results in massive water uptake and dramatic loss of mechanical properties, which could lead to weakness or a dimensional mismatch when incorporated into a membrane electrode assembly (MEA) [12]. Formation of hydrophilic domains as ionic channels, which facilitate the transportation of protons through membranes, is an effective approach to develop highly proton-conductive PEMs. Several methods to perform this strategy have been reported, such as development of phase-separation with block copolymers [13–15], introduction pendant or branched sulfonic acid groups to PEMs [16,17], and controls of sulfonic group's position and concentration [18–21]. Among them, the locally and densely sulfonated aromatic polymers are of special interest due to the large differences in polarity between hydrophilic units and hydrophobic backbones enable the formation of well-defined nanophase-separated structures. For example, Hay et al. reported the synthesis of a sulfonated poly(aryl ether) containing randomly distributed nanoclusters of six sulfonic acid groups. These copolymers possessed good phase-separated morphological structure and relatively high proton conductivity [18]. Ueda et al. reported locally sulfonated poly(ether sulfone)s with eight sulfonic acid groups in each repeat unit, which exhibited the same level of proton conductivity as that of Nafion® 117 in the range of 30–95% RH at 80 °C [19]. However, now the research on the precise control of nanoscale morphology of polymers to improve proton conduction is still a challenge.

In this report, we design and synthesize a novel bisphenol monomer, phenolphthalein derivative **5**, with the rigid and bulky tetraphenylmethane groups, which contain a number of pendant phenyl rings providing the selective sulfonation sites. After post sulfonation, the five sulfonic acid groups are introduced in both parent and pendant phenyl groups of each PPH-containing unit. The introduction of rigid and bulky tetraphenylmethane groups allow for the formation of a well-defined phase-separated structure, improving the nanophase separated morphology of PEMs which could be expected to be beneficial for proton transport. Moreover, the more PPH derivatives can provide more free volume in membranes which will result in more water molecules being confined [22,23]. Especially, steric size matching of tetraphenylmethane groups and PPH molecule can benefit enlarging free volume to increase water uptake in premise of maintaining comparatively low swelling ratio (Fig. 1). The synthesis and property of this new series of PEMs are investigated in detail and the water uptake, methanol permeability, proton conductivity and cell performance are determined. It is noted that SPES-20 exhibited the good single-cell performance in a DMFC which was superior to that of Nafion® 117.

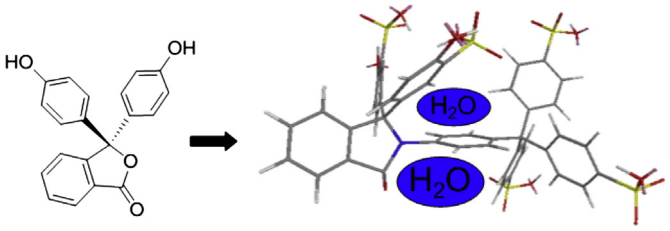

Fig. 1. PPH Molecule and steric size matching PPH derivatives in which water molecules are trapped.

2. Experimental section

2.1. Materials

Phenolphthalein was purchased from Beijing Chemical Reagent Company. 1-Methyl-2-pyrrolidinone (NMP) was dried with CaH_2 and distilled under reduced pressure before use. 4-Tritylaniline hydrochloride **3** was synthesized from triphenylmethylchloride and aniline according to the previous report [24]. All other chemicals were reagent grade and used as received.

2.2. Synthesis of dihydrophenolphthalein **2**

Phenolphthalein **1**(50 g, 157 mmol) was dissolved in a solution of sodium hydroxide (12.9 g, 322 mmol) in water (500 mL), and sodium borohydride (23.8 g, 628 mmol) was added. The reaction mixture was stirred at room temperature for 12 h. The reaction mixture was acidified with 4 M HCl to pH 3, and the resulting white precipitate was collected and washed with 100 mL × 3 water. The white solid was dried *in vacuo* to yield 50.2 g (96%) of the desired product as a white solid.

^{1}H NMR (300 MHz, DMSO; ppm): δ 9.28 (br, 2H), 7.71 (d, 1H, J = 9.0 Hz), 7.41 (t, 1H, J = 6.0 Hz), 7.27 (t, 1H, J = 6.0 Hz), 6.97 (d, 1H, J = 6.0 Hz), 6.78 (d, 4H. J = 9.0 Hz), 6.66 (d, 4H, J = 9.0 Hz), 6.38 (s, 1H); ^{13}C NMR (75 MHz, DMSO; ppm): δ 169.5, 155.9, 145.4, 134.8, 131.9, 131.3, 130.6, 130.4, 130.2, 126.3, 115.7, 50.0.

2.3. Synthesis of compound **4**

To a solution of dihydrophenolphthalein **2** (16 g, 50 mmol), 4-tritylbenzenamine (18.6 g, 50 mmol) and DIPEA (13.5 g, 105 mmol) in anhydrous DMF (120 mL) was added HATU (20.9 g, 55 mmol), and the solution was stirred at room temperature for 12 h. The reaction mixture was diluted with water (50 mL) and the insoluble solid filtered and washed with 100 mL water. The crude product **4** (30.3 g, 95%) was obtained and used for the next step directly without further purification.

^{1}H NMR (300 MHz, DMSO; ppm): δ 10.3 (s, 1H), 9.24 (s, 2H), 7.55 (d, 2H, J = 9.0 Hz), 7.40 (t, 2H, J = 9.0 Hz), 7.28–7.33 (m, 7H), 7.15–7.23 (m, 9H), 7.07 (d, 3H, J = 6.0 Hz), 6.84 (d, 4H. J = 9.0 Hz), 6.64 (d, 4H, J = 6.0 Hz), 5.85 (s, 1H); ^{13}C NMR (75 MHz, DMSO; ppm): δ 168.3, 155.8, 146.9, 142.9, 141.9, 137.7, 137.4, 134.6, 131.1, 130.9, 130.4, 128.1, 126.4, 119.6, 115.5, 64.5, 50.5.

2.4. Synthesis of compound **5**

Compound **5** was synthesized according to the method reported by M. Adamczyk's group [25].

To a solution of compound **4** (28.67 g 45 mmol) in methanol (200 mL) was added dichlorodicyanoquinone (DDQ, 21.5 g, 90 mmol). The reaction was stirred for 24 h at ambient temperature. Purified by column separation to get the desire product as a yellow solid (yield: 90%).

^{1}H NMR (300 MHz, DMSO; ppm): δ 9.62 (s, 2H), 7.82 (d, 1H, J = 9.0 Hz), 7.60 (t, 1H, J = 9.0 Hz), 7.51 (t, 1H, J = 9.0 Hz), 7.17–7.32 (m, 10H), 7.03 (d, 6H, J = 6.0 Hz), 6.90 (d, 6H. J = 9.0 Hz), 6.82 (d, 2H, J = 9.0 Hz), 6.64 (d, 4H, J = 9.0 Hz); ^{13}C NMR (75 MHz, DMSO; ppm): δ 168.3, 157.4, 152.3, 146.5, 145.3, 135.6, 133.4, 130.9, 129.8, 128.1, 127.4, 126.5, 124.5, 124.0, 115.3, 78.0, 64.5. ESMS: 636.3 $(M + H)^+$.

2.5. Synthesis of PES-x

A typical synthetic procedure for PES-25 is illustrated as follows: compound **5** (0.794 mg, 1.25 mmol), compound **6** (937.5 mg, 3.75 mmol), bis(4-fluorophenyl)sulfone (1.27 g, 5 mmol), K_2CO_3 (897 mg, 6.5 mmol), NMP (10 mL) and toluene (10 mL) were added into a 100 mL three-neck flask equipped with a mechanical stirrer, a Dean_Stark trap, and a nitrogen inlet. The reaction mixture was kept at 140 °C for 4 h to give a viscous solution. After 4 h, the toluene was removed from the reaction by slowly increasing the temperature to 170 °C, and then the reaction was allowed to continue for another 8 h. The mixture was cooled to room temperature and diluted with NMP. The solution was poured into 500 mL of deionized water with vigorous stirring. The resulting product was washed with deionized water and hot methanol several times and dried at 80 °C under vacuum for 24 h. Yield: 98%.

Other polymers were prepared by the same method described above. The obtained polymers are denoted by PES-*x*, where *x* refers to the mole fraction of the monomer **5** in the feed.

2.6. Typical synthetic procedure for the synthesis of SPES-x

Polymers PES-*x* reacted with chlorosulfonic acid in CH_2Cl_2 to give the title sulfonated polymers SPES-*x*. The following description will be focused on SPES-25.

A solution of chlorosulfonic acid (2.5 mL) in dichloromethane (60 mL) was placed in a round-bottomed flask. A solution of the polymer PES-25 (1.8 g) in dichloromethane (60 mL) was added dropwise to the solution of chlorosulfonic acid in dichloromethane with stirring. The sulfonation reaction was allowed to proceed for 4 h until all of the sulfonated polymers had precipitated from the reaction mixture. The product was poured into cold water (500 mL) and filtered. The isolated white polymers were washed with deionized water several times before being dried under vacuum at 80 °C overnight. Yield: 97%.

2.7. Membrane preparation

The sulfonated copolymers were cast onto glass plate from their DMAc solution (5–7 wt.%) after filtration. The removal of DMAc was accomplished in an oven at 60 °C for 8 h and then at 120 °C under vacuum for 10 h. The polymer membranes were treated with 1.0 N sulfuric acid at room temperature for 2 days, followed by thoroughly washed with deionized water and then dried under vacuum at 100 °C for 10 h. Tough, ductile ionomer membranes were obtained with a controlled thickness of 30–50 μm.

2.8. Measurements

^{1}H NMR spectra were measured at 300 MHz on an AV 300 spectrometer. Thermogravimetric analysis (TGA) was performed in air atmosphere on a TA Instrument TGA Q500 thermogravimetric analyzer from 50 to 800 °C at a heating rate of 10 °C min^{-1}. Tensile measurements were conducted with an Instron-1211 at a speed of 1 mm min^{-1} at room temperature and ambient humidity conditions. The size of samples was 20 × 5 mm. For TEM observations, the membranes were stained with lead ions by ion exchange of the sulfonic acid groups in 1 wt.% $Pb(OAc)_2$ aqueous solution for 2 days, rinsed with deionized water and then dried at room temperature for 2 days.

The water uptake and swelling ratio were determined by measuring the difference in weight and length between dry and hydrated membranes.

Water uptake of the membranes was calculated from Equation (1):

$$\text{Water uptake}(\%) = [(W_w - W_d)/W_d] \times 100 \quad (1)$$

where W_d and W_w are the weights of dry and corresponding water-swollen membranes, respectively.

Water swelling ratio of the polymer membranes was calculated from Equation (2):

$$\text{Swelling ratio}(\%) = [(l_w - l_d)/l_d] \times 100 \quad (2)$$

where l_d and l_w are the diameters of dry and wet membranes, respectively.

The oxidative stability of SPES-*x* membranes was evaluated by changes in molecular weight of membranes after they were soaked in Fenton's reagent (3% H_2O_2 containing 2 ppm $FeSO_4$) at 80 °C for 1 h.

The proton conductivity (σ, S cm^{-1}) of each membrane coupon (size: 1 cm × 4 cm) was obtained using $\sigma = d/\text{LsWs}R$ (d is the distance between the adjacent electrodes, and Ls and Ws are the thickness and width of the membrane, respectively). The resistance value (R) was measured over the frequency range of 100 mHz–100 KHz by four-point probe AC impedance spectroscopy using an electrode system connected with an impedance/gain-phase analyzer (Solatron 1260) and an electrochemical interface (Solatron 1287, Farnborough Hampshire, ONR, UK). The membranes were sandwiched between two pairs of gold-plate electrodes. The membranes and the electrodes were set in a Teflon cell and the distance between the adjacent electrodes was 1 cm. The cell was placed in a thermo-controlled chamber in deionized water for measurement. At a given temperature, the samples were equilibrated for at least 30 min before measurements. Repeated measurements were taken at the desired temperature with 10-min interval until no more change in conductivity was observed.

The methanol permeability was determined by using a cell consisting of two half-cells separated by the membrane, which was fixed between two rubber rings. Methanol (2 mol L^{-1}) was placed on one side of the diffusion cell, and deionized water was placed on the other side. Magnetic stirrers were used in each compartment to ensure uniformity. The concentration of methanol was measured by a SHIMADZU GC-1020A series gas chromatograph. Peak areas were converted into methanol concentration with a calibration curve. The methanol permeability was calculated by Equation (3):

$$C_B(t) = \frac{A}{V_B} \cdot \frac{DK}{L} \cdot C_A \cdot (t - t_0) \quad (3)$$

where C_A and C_B are the methanol concentration in feed and in permeate, respectively. A, L and V_B are the effective area, the thickness of membrane and the volume of permeated compartment, respectively. DK is defined as the methanol permeability and t_0 is the time lag.

Small angle X-ray scattering was measured for SPES-*x* membranes at 50% RH and room temperature. The range of scattering vectors explored ($q = 4\pi\sin 2\theta/\lambda_i$) was from 0.08 to 3.0 nm^{-1}, where λ_i and 2θ are the incident wavelength and total scattering angle, respectively.

The membrane electrode assembly (MEA) with SPES-20 and Nafion® 117 membranes was made according to the literature method [26]. A slurry which consisted of Vulcan XC-72 carbon and PTFE (20 wt.%) was coated onto the carbon paper (TGPH060, 20 wt.% PTFE, Toray) to form the cathodic microporous layer (MPL). The XC-72 carbon loading was ca. 2 mg cm^{-2}. For the preparation of anodic MPL, a slurry consisting of carbon materials and PTFE (20 wt.%) was coated onto the carbon paper (TGPH060, 0 wt.% PTFE, Toray) to form the anodic MPL. The total carbon

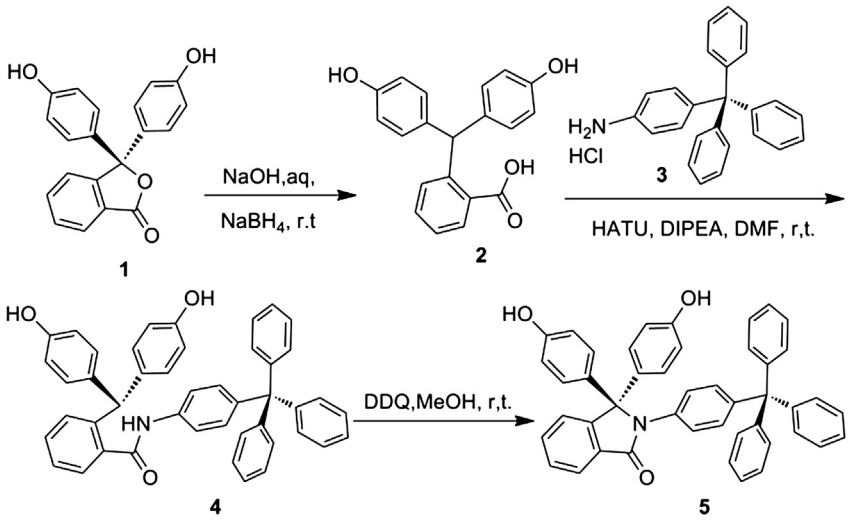

Scheme 1. Synthesis of the monomer **5**.

loading was ca. 1 mg cm^{-2}. The anode and cathode catalysts used in this work were Pt–Ru black with an atomic ratio 1:1 (HiSpec 6000, Johnson Matthey) and carbon-supported Pt with a Pt loading of 60 wt.% (HiSpec 9000, Johnson Matthey), respectively. Catalyst ink was prepared by dispersing appropriate amount of catalyst and 5 wt.% Nafion solution (Aldrich) into a mixture of isopropyl alcohol and ultrapure water with a volume ratio of 1:1. The catalyst ink was then sprayed on the MPL. The metal loading was 4.0 ± 0.2 mg cm^{-2} for both cathode and anode, and the ionomer loading was 20 wt.% for the cathode and 15 wt.% for the anode, respectively. The membrane electrode assemblies were prepared by hot-pressing both anode and cathode on both sides of Nafion@ 117 and SPES-20 membrane at 6 MPa for 3 min at 130 °C and 150 °C, respectively. The polarization curves of the passive DMFCs at room temperature were obtained on an Arbin FCT testing system (Arbin Instrument Inc. USA) by using 4 M methanol aqueous solution as fuel. At each discharging current point along the polarization curve, a 2 min waiting period was kept to obtain a stable voltage reading.

3. Results and discussion

3.1. Synthesis of monomer and sulfonated copolymers

The new bisphenol monomer **5** was readily prepared from phenolphthalein and 4-tritylaniline by the modified reaction sequences in three steps [25]. Scheme 1 shows the synthetic route of monomer **5**. The desired product was obtained in 82% total yield based on phenolphthalein and the structure was confirmed by ^{1}H NMR spectra. As shown in Fig. 2, the –OH signal appeared at 9.62 ppm. The clean peaks of aromatic protons H_1 to H_{11} confirmed the structure of the new monomer **5**.

The novel cardo poly(arylene ether sulfone) copolymers containing rigid and bulky hydrophobic components were synthesized by the copolymerization of new bisphenol monomer **5** and bis(4-hydroxyphenyl) sulfone with 4,4,-difluorophenyl sulfone under nucleophilic aromatic substitution conditions. The copolymers were further sulfonated with chlorosulfonic acid in dichloromethane solution at room temperature, provided the desired SPES-

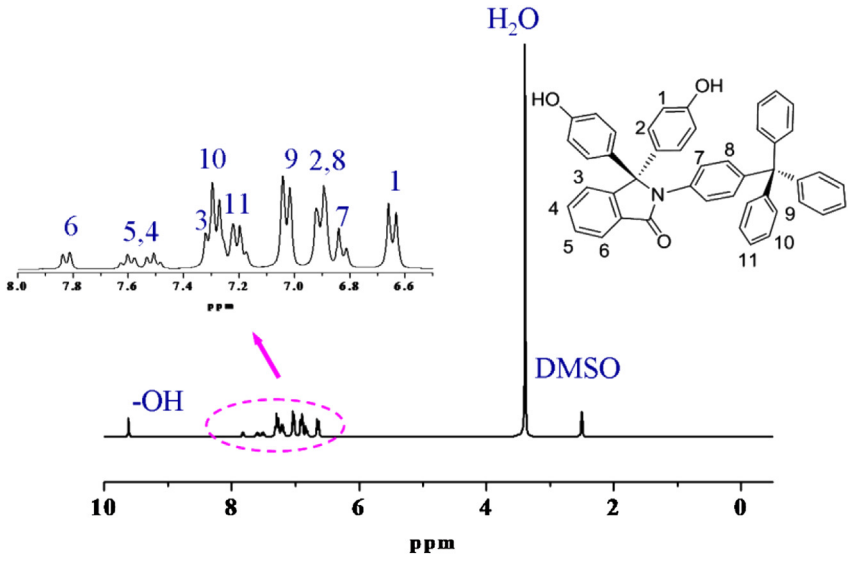

Fig. 2. ^{1}H NMR spectrum of bisphenol monomer **5**.

x in good yield (Scheme 2). In order to achieve the completely sulfonation of SPES-*x*, it is necessary to use excess chlorosulfonic acid. The chemical structures of SPES-*x* were confirmed by ^{1}H NMR spectra. As expected, the −OH proton signal at 9.62 ppm, H_3 and H_{11} proton signals at 6.90 and 7.31 ppm disappeared completely, while new signals for neighbors of the sulfonic acid groups appeared at 7.55 ppm (Fig. 3). No partial sulfonated copolymer signals could be observed in ^{1}H NMR spectra, which suggested that the sulfonation reaction was complete. Furthermore, in order to confirm the certain site of the sulfonic acid groups in sulfonated copolymers, we prepared model compound **8** by using compound **5** as starting materials through methylation which were further sulfonated with chlorosulfonic acid to get compound **9** (Fig. S1). The chemical structure of compound **9** was identified by ^{1}H NMR stacked spectra (Fig. S2).

The structure of copolymers SPES-*x* was also confirmed by IR spectroscopy (Fig. S3). The IR spectra showed that the carbonyl group at 1689 cm^{-1} was observed for all SPES-*x*. The characteristic absorptions of the symmetric and asymmetric stretching vibrations of $-SO_3H$ appeared at 1160 and 1033 cm^{-1}, respectively.

The intrinsic viscosities and solubility of the copolymers were listed in Table S1. The viscosity values of these copolymers are in range of 0.33–0.79 dL g^{-1}, which indicated the polymerizations were carried out successfully. The sulfonated polymers were readily soluble in polar solvents such as DMF, DMAc, NMP, and DMSO, and afforded flexible and transparent films by polymer solution casting. When the content of monomer **5** in the bisphenol was higher than 40%, the intrinsic viscosities of polymers were obviously decreased. The nucleophilic substitution reaction process was more difficult due to the large steric hindrance of rigid tetraphenylmethane groups.

3.2. Thermal and mechanical properties

The thermal stabilities of the polymers were investigated by TGA. The TGA curves of SPES-*x* in air atmosphere as shown in Fig. 4 exhibited a typical three-step degradation pattern. The initial degradation step observed at room temperature to ca. 200 °C, can be associated with the loss of water molecules, absorbed by the highly hygroscopic $-SO_3H$ groups. The second weight loss step starting at about 260 °C was assigned to the thermal degradation of

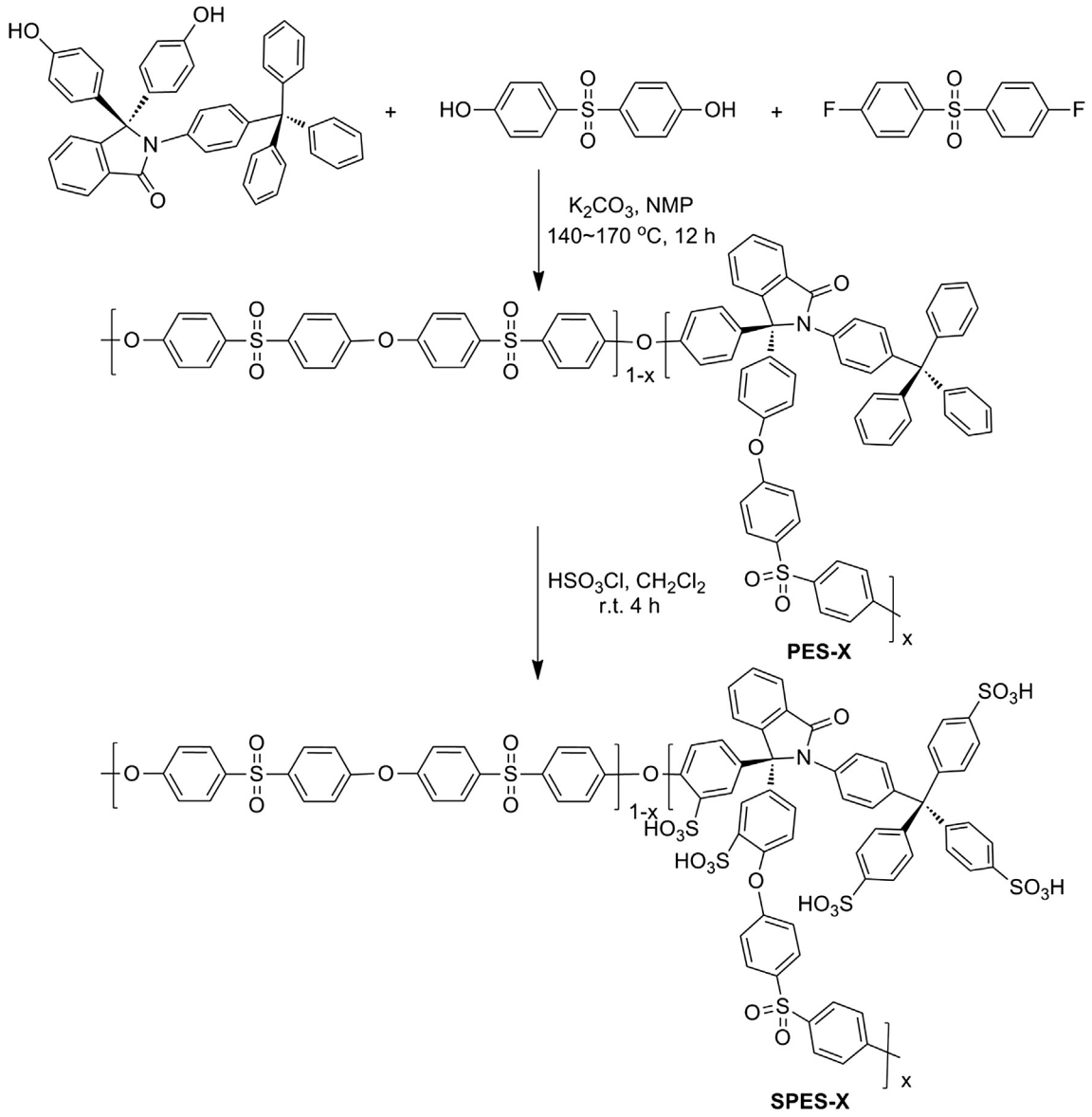

Scheme 2. Synthesis of side-chain-type copolymers SPES-*x*.

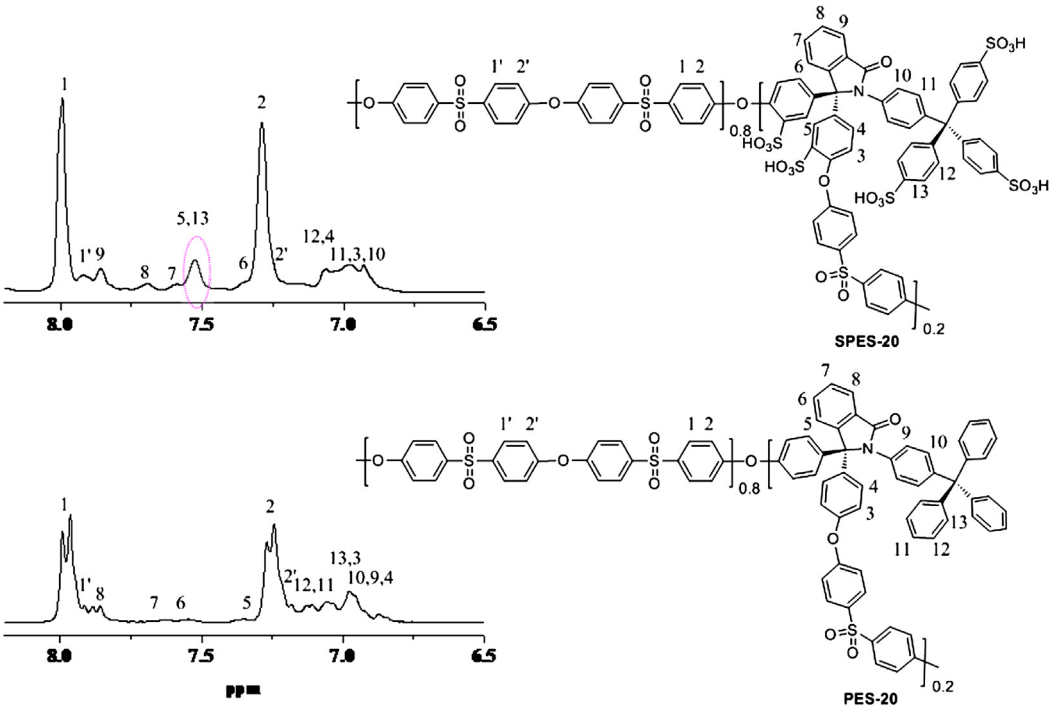

Fig. 3. ^{1}H NMR spectra of SPES-20 and PES-20.

sulfonic acid groups, while the third step observed at around 400 °C can be attributed to the decomposition of the main polymer chain.

Mechanical properties of SPES-*x* were summarized in Table 1. The SPES-*x* membranes showed good mechanical properties with tensile modulus in the range of 0.78–1.25 GPa, elongations at break of 9.1–18.3%, and tensile strength at break of 21.4–41.8 MPa. These results indicate that the tensile strength of membrane SPES-*x* weakens along with the increasing of content of monomer **5**. It is noted that the tensile strength membrane SPES-30 is still higher than 20 MPa to ensure necessary mechanical strength.

3.3. Morphology of membranes

Proton conductivity of the membranes is closely related to their morphology. TEM images of SPES-*x* membranes are shown in Fig. 5.

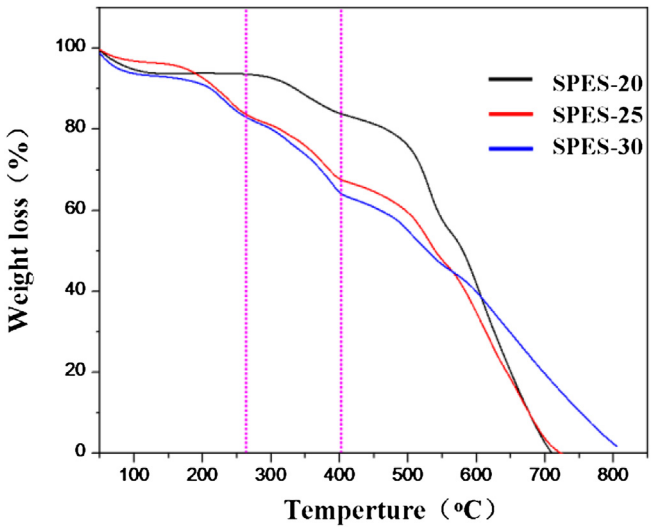

Fig. 4. TGA curves of the SPES-*x* membranes in air atmosphere.

The dark domains represent hydrophilic domains (ionic clusters) due to Pb^{2+} staining, and lighter regions represent hydrophobic domains. All these membranes showed well-defined phase-separated structures and well-interconnected spherical ionic channels.

As clearly seen in Fig. 5, the phase separation was more distinct with the higher IEC values. For SPES-20 membrane with the lowest IEC of 1.57 mequiv g^{-1}, only small, dense and uniform ion clusters could be observed (Fig. 5a). The higher IEC (1.85 mequiv g^{-1}) in SPES-25 caused the formation of bigger spherical ionic clusters (about 2.0–5.0 nm in diameter) (Fig. 5b) and the connectivity of these ionic clusters was significantly improved. For SPES-30 membrane with the highest IEC of 2.08 mequiv g^{-1}, the well-defined and connected ionic channels in the size range of 4–10 nm (Fig. 5c) were observed. The morphology should be caused by the large difference in polarity between the locally and densely sulfonated hydrophilic units and the hydrophobic backbones, which was expected to provide an effective proton transport through hydrophilic ionic channels.

The microstructures of these membranes were further characterized by SAXS. As shown in Fig. 6, the corresponding SAXS profiles exhibited a clear peak for all SPES-*x* membranes. This result indicated that phase separation between the hydrophilic units and the hydrophobic backbones was locally correlated. Moreover, accordingly the *q* values of the ionomer peak shift to low values with increasing content of **5**. This suggested that the characteristic separation lengths between ion-rich domains and the hydrophobic

Table 1
Mechanical property of SPES-*x*.

Sample[a]	Tensile strength (MPa)	Young's modulus (MPa)	Elongation at break (%)
SPES-20	41.8	1250	18.3
SPES-25	35.6	947	15.0
SPES-30	21.4	784	9.1

[a] Samples were dried at ambient conditions for one day and tested at 30 °C, and ambient humidity conditions.

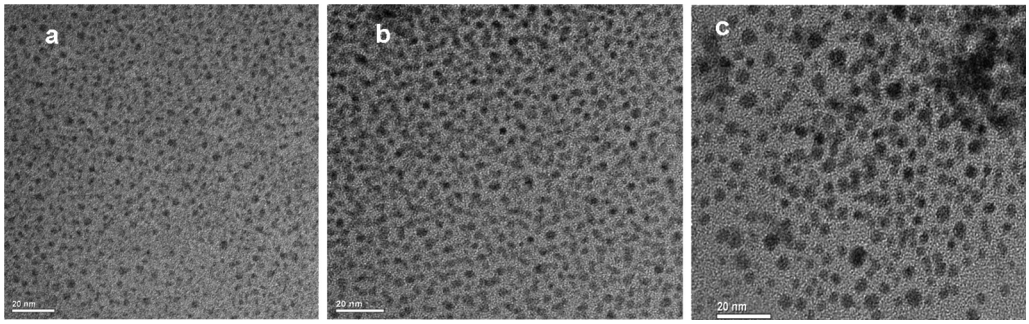

Fig. 5. TEM images of (a) SPES-20 (IEC = 1.61 mequiv g^{-1}), (b) SPES-25 (IEC = 1.89 mequiv g^{-1}), (c) SPES-30 (IEC = 2.14 mequiv g^{-1}).

polymer-rich domains increase with the increasing concentrations of sulfonic acid groups, which was in good agreement with the TEM results. The values of d for SPES-x membranes, calculated from $d = 2\pi/q$, were in the range of 4.8–6.0 nm, which were larger than that of Nafion® 117 (d = 3.4 nm) [27]. This large d can facilitate phase separation between hydrophilic and hydrophobic aggregates to form nanochannels for efficient proton-transport.

3.4. IEC, water uptake, swelling ratio and proton conductivity

IEC represents the amount of exchangeable protons in ionomer membranes. The IEC values were determined by a titration method, which were close to the theoretical values, indicating sulfonation for PPH-containing unit was close to a quantitative reaction (Table 2). In addition, the content of the sulfonic acid groups in the copolymers was exactly controlled through the simple adjustment of the bisphenol monomer feed ratios to achieve the copolymers with the different IEC values.

Water uptake and swelling ratio have a profound effect on the proton conductivity and mechanical property of PEMs. Water molecules can facilitate proton transport, but excessive water uptake induces unacceptable dimensional changes and a decrease in the mechanical property. Therefore, in order to increase proton conductivities of membranes, properly maintaining the certain level of water content of membranes is necessary on premise of ensuring mechanical properties. Table 2 compares the IEC, water uptake and swelling ratio of copolymer membranes. As shown in Table 2 and Fig. 7, all SPES-x membranes exhibited higher water uptake values than our group previously reported side chain type sulfonated cardo poly(arylene ether sulfone)s bearing aliphatic groups [23] or phenyl groups [28] with the simile IEC values. The highest water uptake was 149% at 80 °C for the highest IEC membrane SPES-30, which corresponds to an absorption of 38.7 (λ) water molecules per sulfonic acid group. The reason of SPES-x membranes maintaining comparatively high water uptake can be attributed to the formation of large and continuous ion networks of sulfonated polymers which was in good agreement with the TEM and SAXS results. As well known, good dimensional stability of membrane is propitious to fabricate MEA of DMFC. SPES-20 and SPES-25 membranes revealed good dimensional stability and the low swelling ratios in the tested temperature range, as shown in Table 2. The largest swelling ratio is about 25%, similar to that of Nafion® 117(23.7%). These properties were distinct from many sulfonated random polymer with similar IECs, which always have an extraordinary raise of dimensional change especially at evaluated temperature [3,15,29,30]. When the value of IEC exceeds 2.10, SPES-x membrane represents obviously dimensional change just when the temperature exceeds 80 °C (Table 2, entry 3). This low swelling ratio of SPES-x membranes with high water uptake can be ascribed to the introduction of rigid and bulky tetraphenylmathane groups in structure. On the one hand, the bulky and rigid tetraphenylmathane groups force each polymer chains apart to provide large interchain separations (free volume) for accommodating water molecules. On the other hand, the steric size matching between two rigid molecules also produces large free volume in which water molecules could be confined. In fact, SPES-x membranes with IEC values over 2.56 mequiv g^{-1} were highly swelled or soluble in water. So the IEC value of 2.1 mequiv g^{-1} is a critical value for SPES-x membranes.

Proton conductivity is a critical property of proton exchange membrane. The proton conductivities of the SPES-x as well as Nafion® 117 were measured in water in the temperature range of 30–80 °C. As shown in Fig. 8, the obtained SPES-x copolymers exhibited proton conductivities above 0.08 S cm^{-1} at 30 °C and their conductivities increased with increasing temperature.

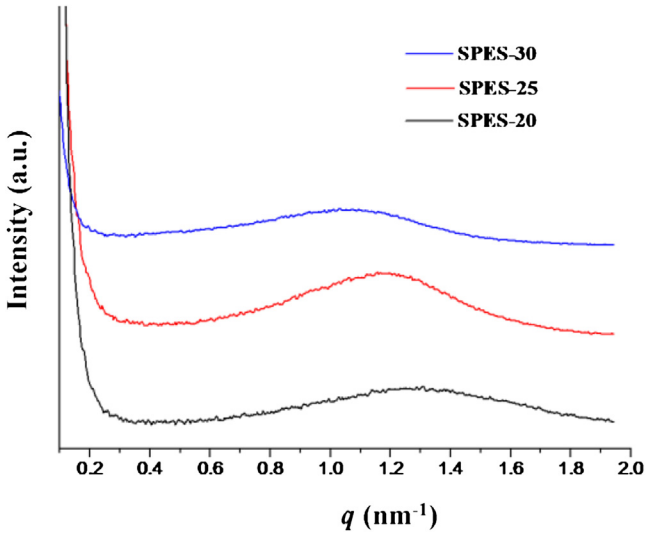

Fig. 6. SAXS data recorded on SPES-x membranes ion-exchanged with lead acetate.

Table 2
The IEC value, water uptake, and swelling ratio of the sulfonated polymers.

Sample	IEC (mequiv g^{-1})		Water uptake (%)		Swelling ratio (%)	
	Theoretical	Experimental[a]	25 °C	80 °C	25 °C	80 °C
SPES-20	1.61	1.57	46.7	70.0	11.9	17.0
SPES-25	1.89	1.85	74.7	89.5	17.7	25.3
SPES-30	2.14	2.08	78.0	149.0	21.0	54.0
Nafion® 117	–	0.91	18.4	34.1	12.6	23.7

[a] IEC from titration.

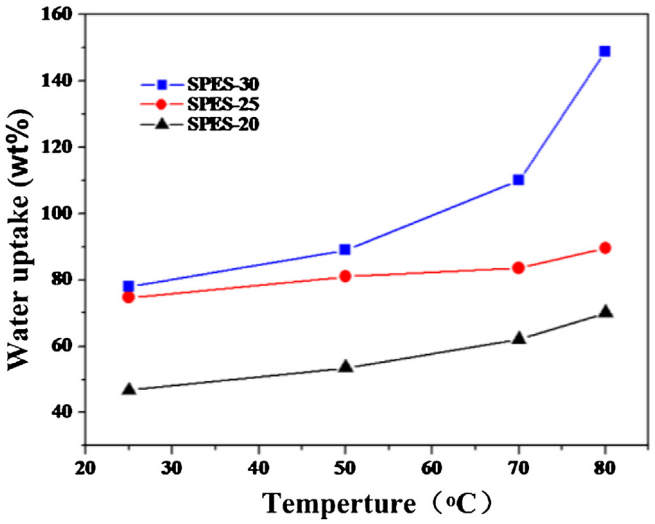

Fig. 7. Temperature dependence of water uptake of the sulfonated polymers.

Compared with 0.072 S cm^{-1} of Nafion@ 117's conductivity, the proton conductivities of SPES-*x* were in the range of 0.088–0.153 S cm^{-1} at 30 °C. Moreover, proton conductivities of SPES-*x* increased from SPES-20 to SPES-30 over the temperature range tested, which indicated conductivities of these polymers were greatly influenced by IEC values. For example, the SPES-30 with the highest IEC showed a proton conductivity of 0.269 S cm^{-1} which was much higher than that of Nafion@ 117 at 80 °C. This high proton conductivity could attribute to its good phase-separated structure which was derived from the large difference in polarity between locally and densely sulfonated units and hydrophobic backbones of polymers. The conductivities of the SPES-*x* membranes also showed an approximate Arrhenius-like temperature dependence. The activation energy (E_a) of conductivity is calculated by fitting the Arrhenius equation $E_a = -b \times R$, where b is the slope of the regression line of ln δ (S cm^{-1}) vs. 1000/T (K^{-1}) and R is the gas constant (8.314 J K^{-1} mol^{-1}). Curves are fitted linearly for E_a determination. The activation energy for proton conduction was found to be in the range of 7.55–15.82 kJ mol^{-1}, which were far smaller than that of the whole aromatic sulfonated polyimide ionomers (21 kJ mol^{-1}) and sulfonated poly(ether ether ketone) ionomers (>30 kJ mol^{-1}) [31,32]. Especially, SPES-20's E_a was 7.55 kJ mol^{-1}, which was lower than that of Nafion@ 117 (11.06 kJ mol^{-1}, reference value being 9.70 kJ mol^{-1}) [33].

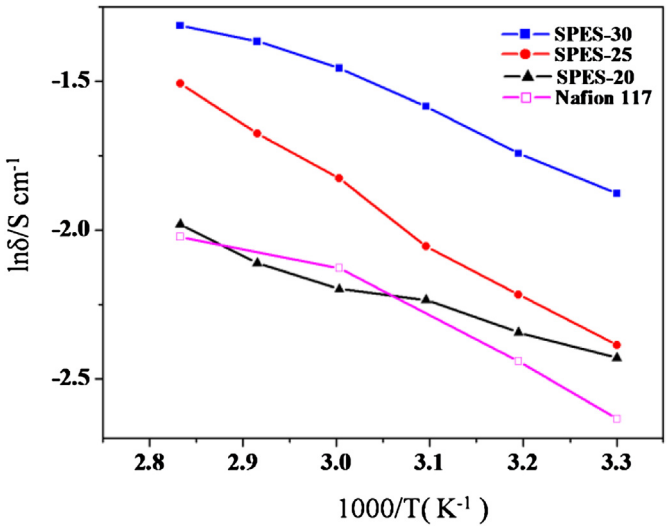

Fig. 8. Arrhenius plots under 100% RH environment for SPES-*x* and Nafion@ 117 membranes.

3.5. Methanol permeation and oxidative stability

Methanol permeation is a key parameter of direct methanol fuel cells (DMFCs) because high methanol permeation will decrease the efficiency of the fuel cell. As summarized in Table 3, the SPES-*x* membranes exhibited low methanol permeability at room temperature, with values in the range of 0.46 × 10^{-6} to 0.98 × 10^{-6} cm^2 S^{-1}, which was lower than the value of Nafion@ 117 of 2.40 × 10^{-6} cm^2 S^{-1}. The selectivity, which was the ratio of proton conductivity (σ) to methanol permeability (P), was often used to estimate the membrane performances. That is to say, the higher the value of σ/P was, the better the performance of the membrane would be. The relative selectivities of copolymers were higher than that of Nafion@ 117 as listed in Table 3.

The oxidative stability of SPES-*x* was evaluated in hot Fenton's reagent for 1 h as an accelerated test. As presented in Table 3, the oxidative stability of these copolymers decreased with an increasing degree of sulfonation. It attributed to comparatively high water uptake of SPES-*x* membranes which was conducive to the attack of hydroxyl radicals for phenylene carbon atoms *ortho* to the ether bonds. Furthermore, these copolymers showed moderate oxidative stability which was comparable to that of fluorene-based sulfonated hydrocarbon polymer [15]. As well known, the latter could be successfully applied in high-temperature fuel cell.

3.6. Single-cell performance

Due to its comparable proton conductivity with Nafion@ 117, good oxidative stability and selectivity, SPES-20 membrane was selected to fabricate MEA and then the electrochemical performance of this new MEA was evaluated. Fig. 9 shows the single cell performance of DMFCs comprising Nafion@ 117 membrane and SPES-20 membrane as polymer electrolytes at 25 °C, including the polarization and power density as a function of the current density. The two passive DMFCs exhibit similar kinetic and ohmic polarization behaviors in a low current density region. In the high current density region, the maximum power density for the passive DMFCs with SPES-20 membrane is 29.4 mW cm^{-2}, which is obviously higher than that with Nafion@ 117 (24.3 mW cm^{-2}) under the same operating conditions. Undoubtedly, MEAs with a SPES-20 membrane show less electrolyte resistance in comparison with that of Nafion@ 117, which is in excellent agreement with the activation energies E_a measured from Fig. 8. To investigate the possible effects of SPES-20 membrane on methanol mass transfer, the passive DMFCs with this membrane as PEM was

Table 3
Methanol permeability and oxidative stability of sulfonated polymer membranes.

Sample	P_M (cm^2 S^{-1}) 10^{-6}	Selectivity (S s cm^{-3}) 10^4	Oxidative stability[a] (wt.%)
SPES-20	0.46	19.1	49
SPES-25	0.76	12.1	40
SPES-30	0.98	15.6	21
Nafion@ 117	2.40	3.75	–

[a] Residue after treatment with Fenton's reagent (3% H_2O_2 aqueous solution containing 2 ppm $FeSO_4$) at 80 °C for 1 h.

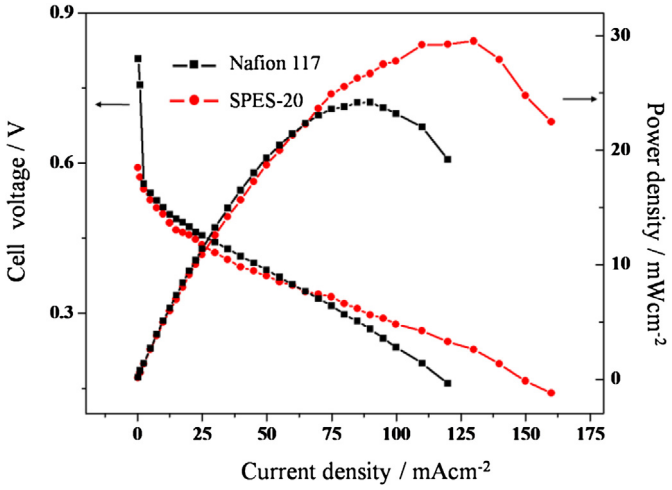

Fig. 9. Cell voltage/power density vs load current-density for DMFC with Nafion@ 117 and SPES-20 membranes.

discharged at a constant voltage of 0.3 V, the cell fueled with 6.0 mL of 3 M methanol. Fig. S4 shows the discharging curves of passive DMFCs. Faradic efficiency (η) and energy efficiency (ξ) for the DMFC with SPES-20 membrane are calculated to be ca. 85.64% and 21.77%, respectively, while those for the DMFC with Nafion@ 117 membrane being 71.20% and 21.10% under same tested conditions [34]. Clearly, when using SPES-20 membrane, the DMFC can reach power density and energy efficiency superior to the best obtained with Nafion@ 117. This high performance of the cell of SPES-20 membrane can be attributed to the much higher selective factor, σ/P, as compared with that of Nafion@ 117 (Table 3). The optimization of the catalysts and the MEA fabrication procedure is in our future agenda for further improving the performance.

4. Conclusions

In summary, a new series of the locally and densely sulfonated cardo poly(arylene ether sulfone)s SPES-*x* with bulky and rigid side chains have been designed and synthesized by a post sulfonation method. The membrane revealed that the introduction of steric size matching rigid tetraphenylmethane groups is favor of the formation of the well-defined phase-separated structure and enhancement of water uptake on the premise of guaranteeing mechanical properties. Moreover, the IEC values could be exactly controlled through the simple adjustment of the bisphenol monomer feed ratios. Experimental results revealed that SPES-20 membrane with high proton conductivity and low methanol permeability exhibits superior single-cell performance compared with Nafion@ 117. Therefore, these novel SPES-*x* membranes with nano-phase separated morphology that has been improved by the introduction of rigid and bulky tetraphenylmethane groups may be the promising PEM materials in fuel cell applications.

Acknowledgments

We thank the National Basic Research Program of China (No. 2012CB932802) and the National Science Foundation of China (No. 51021003, 51133008) for the financial support.

Appendix A. Supplementary data

Supplementary data related to this article can be found at http://dx.doi.org/10.1016/j.jpowsour.2013.07.061.

References

[1] T. Higashihara, K. Matsumoto, M. Ueda, Polymer 50 (2009) 5341–5357.
[2] C.H. Park, C.H. Lee, M.D. Guiver, Y.M. Lee, Prog. Poly. Sci. 36 (2011) 1443–1498.
[3] H.W. Zhang, P.K. Shen, Chem. Rev. 112 (2012) 2780–2832.
[4] Y.L. Liu, Polym. Chem. 3 (2012) 1373–1383.
[5] Y. Yang, S. Holdcroft, Fuel Cells 5 (2005) 171–186.
[6] N.W. Li, C.Y. Wang, S.Y. Lee, C.H. Park, Y.M. Lee, M.D. Guiver, Angew. Chem. Int. Ed. 50 (2011) 9158–9161.
[7] K. Miyatake, Y. Chikashige, M. Watanabe, Macromolecules 36 (2003) 9691–9693.
[8] P.X. Xing, G.P. Robertson, M.D. Guiver, S.D. Mikhailenko, S.J. Kaliaguine, J. Polym. Sci. Part A Polym. Chem. 42 (2004) 2866–2876.
[9] M.M. Guo, B.J. Liu, L. Li, C. Liu, L.F. Wang, Z.H. Jiang, J. Power Sources 195 (2010) 11–20.
[10] B.R. Einsla, Y.T. Hong, Y.S. Kim, F. Wang, N. Gunduz, J.E. McGrath, J. Polym. Sci. Part A Polym. Chem. 42 (2004) 862–874.
[11] S.H. Tian, D. Shu, S.J. Wang, M. Xiao, Y.Z. Meng, J. Power Sources 195 (2010) 97–103.
[12] M. Schuster, C.C. de Araujo, V. Atanasov, H.T. Andersen, K.-D. Kreuer, J. Maier, Macromolecules 42 (2009) 3129–3137.
[13] Y.A. Elabd, M.A. Hickner, Macromolecules 44 (2011) 1–11.
[14] R.L. Guo, O. Lane, D. VanHouten, J.E. McGrath, Ind. Eng. Chem. Res. 49 (2010) 12125–12134.
[15] B.H. Bae, T.S. Yoda, K.J. Miyatake, H. Uchida, M. Watanabe, Angew. Chem. Int. Ed. 49 (2010) 317–320.
[16] D.S. Kim, Y.S. Kim, M.D. Guiver, J.F. Ding, B.S. Pivovar, J. Power Sources 182 (2008) 100–105.
[17] S. Matsumura, A.R. Hlil, C. Lepiller, J. Gaudet, D. Guay, Z. Shi, S. Holdcroft, A.S. Hay, Macromolecules 41 (2008) 281–284.
[18] S. Matsumura, A.R. Hlil, C. Lepiller, J. Gaudet, D. Guay, A.S. Hay, Macromolecules 41 (2008) 277–280.
[19] K. Matsumoto, T. Higashihara, M. Ueda, Macromolecules 42 (2009) 1161–1166.
[20] F.X. Gong, S.B. Zhang, J. Power Sources 196 (2012) 9876–9883.
[21] S.N. Feng, K.Z. Shen, Y. Wang, J.H. Pang, Z.H. Jiang, J. Power Sources 224 (2013) 42–49.
[22] Q. Zhang, F.X. Gong, S.B. Zhang, S.H. Li, J. Membr. Sci. 367 (2011) 166–173.
[23] N. Gao, F. Zhang, S.B. Zhang, J. Liu, J. Membr. Sci. 372 (2011) 49–56.
[24] P. Ganesan, X.N. Yang, J. Loos, T.J. Savenije, R.D. Abellon, H. Zuilhof, E.J.R. Sudhölter, J. Am. Chem. Soc. 127 (2005) 14530–14531.
[25] M. Adamczyk, J. Grote, Org. Prep. Proced. Int. 33 (2001) 95–100.
[26] M. Chen, J. Chen, Y. Li, Q.H. Huang, H.F. Zhang, X.Z. Xue, Z.Q. Zou, H. Yang, Energy Fuels 26 (2012) 1178–1184.
[27] G. Gebel, Polymer 41 (2000) 5829–5838.
[28] Our unpublished results: the water uptake of new phenyl substituted copolymers is 20.1%.
[29] K. Nakabayashi, T. Higashihara, M. Ueda, Macromolecules 43 (2010) 5756–5761.
[30] P.X. Xing, G.P. Robertson, M.D. Guiver, S.D. Mikhailenko, S. Kaliaguine, Macromolecules 37 (2004) 7960–7967.
[31] K. Miyatake, H. Zhou, H. Uchida, M. Watanabe, Chem. Commun. (2003) 368–369.
[32] L. Li, J. Zhang, Y.X. Wang, J. Membr. Sci. 226 (2003) 159–167.
[33] J.H. Pang, H.B. Zhang, X.F. Li, L.F. Wang, B.J. Liu, Z.H. Jiang, J. Membr. Sci. 318 (2008) 271–279.
[34] T. Yuan, Z.Q. Zou, M. Chen, Z.L. Li, B.J. Xia, H. Yang, J. Power Sources 192 (2009) 423–428.